MEASUREMENT OF CP ASYMMETRIES AT BELLE

William Trischuk*
Department of Physics
University of Toronto, Toronto, Ontario,
M5S 1A7, Canada

Representing the Belle Collaboration

ABSTRACT

The Belle experiment at the KEK B factory has collected 93 fb^{-1} of electron positron collisions at $\sqrt{s} = 10.6$ GeV. This has produced a sample of 85 million $B\bar{B}$ meson pairs that can be used to study CP violation in rare (and not so rare) B decay modes. Here I report on a measurement of indirect CP violation in the decay $B^0 \to J/\psi K^0_S$, as well as time dependent CP asymmetries in rarer modes such as $B^0 \to \pi^+\pi^-, \eta' K^0_S$ and ϕK^0_S. I summarise the prospects for improving the precision on these and related measurements.

*With support from Princeton University and the Japanese Accelerator Laboratory, KEK.

1 CP Violation in B Decay

When CP violation was first observed in neutral kaon decay, in the early 1960s, it shook the foundations of particle physics. It had previously been assumed that the combination of charge conjugation and a parity transformation left all known particle interactions invariant, despite the fact that weak interactions violated parity alone. Over the following three decades CP violation in the K^0 system was measured with ever increasing precision in an attempt to pin down its source. In the 1970s Kobyashi and Maskawa[1] showed that the Standard Model could accommodate some CP violation in a three quark weak mixing matrix, V_{CKM}. However the single phase necessary to parametrise this 3×3 unitary matrix produced a small effect in K^0 meson decay, where CP violation was observed at the 10^{-3} level. It was suggested,[2] in the early 1980s, that the comparable amplitudes for the direct decay of B^0 mesons into CP eigenstates and the mixing of $B^0\bar{B}^0$ mesons would make neutral B meson decay an ideal place to observe large CP violating effects.

One way to understand the relative magnitude of CP violation predicted by the CKM model in neutral B meson decay is to consider the unitarity relation between the first and third columns of V_{CKM}:

$$V_{tb}^* V_{td} + V_{cb}^* V_{cd} + V_{ub}^* V_{ud} = 0$$

While each term in term in this expression is relatively small ($\mathcal{O}(\sin^3 \theta_C)$), they are all the same size. When plotted in the complex plane (see fig. 1) one expects significant angles at each apex because the three sides of the triangle have similar lengths. In neutral kaon decay the corresponding unitarity triangle has two sides that are much larger than the third – making the decay rates for K^0 mesons much larger, but making the angles, and hence the observable phases small and thus difficult to measure.

In B meson decay CP violating phases are most readily observable through the indirect mixing of two amplitudes. Given a CP eigenstate accessible to both B^0 and $\bar{B}^0$ decays – such as $J/\psi K_S^0$ – one can measure the interference between the direct decay amplitudes:

$$B^0(\bar{B}^0) \to J/\psi K_S^0$$

and the amplitude for the same decay preceded by B^0 mixing:

$$B^0(\bar{B}^0) \to \bar{B}^0(B^0) \to J/\psi K_S^0$$

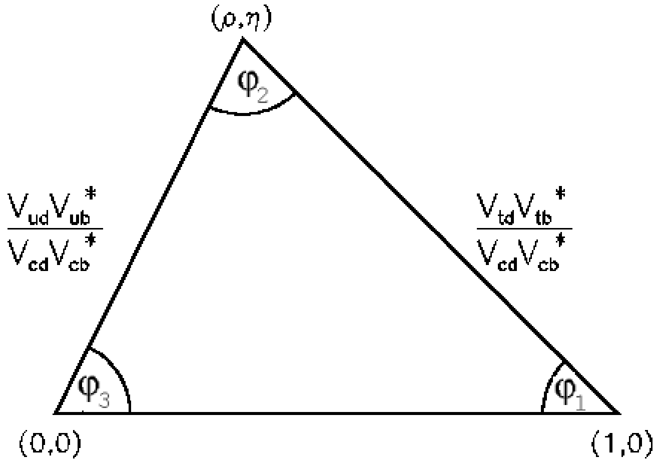

Figure 1: Unitarity of the CKM matrix inter-relates different elements. For the study of CP violation in B meson decay the most useful relationship can be depicted graphically in this triangular relationship.

When one includes the relative phase between these two amplitudes we get at an expression for the time dependent CP asymmetry:

$$\begin{aligned} A_{CP}(\Delta t) &\equiv \frac{\frac{dN}{dt}(\bar{B}^0 \to J/\psi K_\xi) - \frac{dN}{dt}(B^0 \to J/\psi K_\xi)}{\frac{dN}{dt}(\bar{B}^0 \to J/\psi K_\xi) + \frac{dN}{dt}(B^0 \to J/\psi K_\xi} \\ &= -\ \xi_K \sin\ 2\phi_1\ \sin\ \Delta m \Delta t \qquad [1] \end{aligned}$$

Where the asymmetry in the decay rate between B^0 and $\bar{B}^0$ mesons is related to the B^0 mixing rate ($\sin \Delta m \Delta t$), the CP eigenvalue of the final state, ξ_K, ($\xi_K = -1$ for $J/\psi K_S^0$ final states and $+1$ for $J/\psi K_L^0$ final states) and $\sin 2\phi_1$, the angle at the lower right apex of the unitarity triangle shown in fig. 1.

2 The KEK-B Collider and Belle Detector

The experimental challenge in observing CP violation in B meson decay lies in the fact that the B mesons decay much more quickly than K mesons having proper flight distances of fractions of a millimeter, versus meters. Furthermore the decay rate to experimentally accessible CP eigenstates are very much smaller: $\mathcal{O}(10^{-4})$ for B mesons; while essentially 100% of neutral K meson decays are to identifiable CP eigenstates. While the very much larger CP violation in B decay makes up for some of this it remained a significant experimental challenge to observe CP violation in B meson decay.

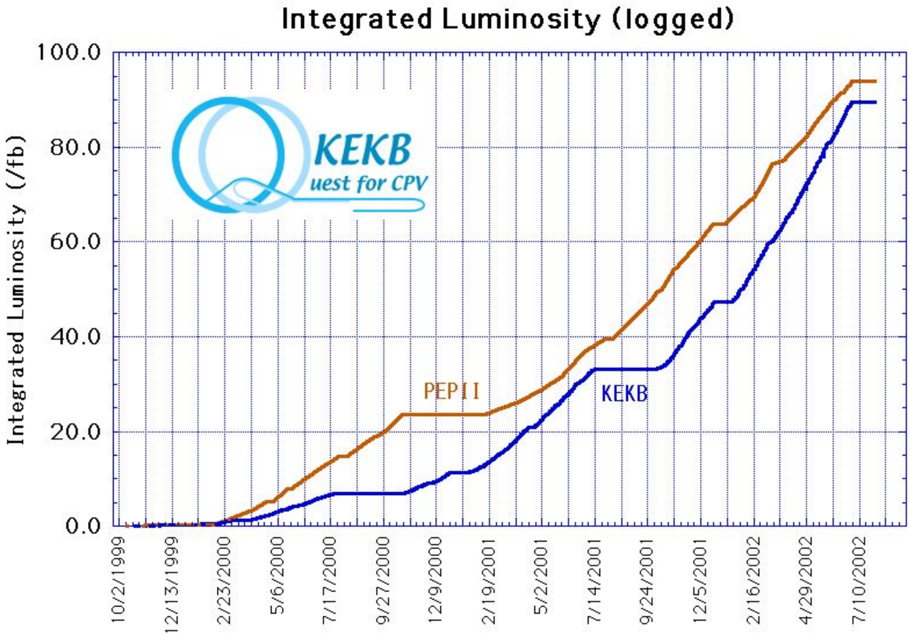

Figure 2: The Belle experiment has been collecting data over the last two years. This plot shows the rate of integrating luminosity over that period (lower line) compared to the luminosity collected by the BaBar experiment at PEPII (upper line). The data sample sizes are similar at this point.

The key ingredient to this observation is having a high luminosity source of B mesons, a B factory. Two dedicated machines were built in the late 1990s to address this problem. The KEK-B e^+e^- collider uses beams of 8 GeV electrons and 3.5 GeV positrons, to produce $\Upsilon(4S)$ mesons at 10.6 GeV. These, in turn, decay into $B\bar{B}$ meson pairs. Using an 11 mrad crossing angle KEK-B is able to collide beams with currents in excess of 1 Ampere, with tolerable backgrounds for the experiment, producing luminosities approaching 10^{34} per cm^2 each second. An integrated luminosity comparison between the KEK-B factory and its competitor PEP-II at SLAC is shown in fig. 2. While the two machines have delivered similar integrated luminosities since they came online two years ago, the recent instantaneous luminosities (the slope of the curve) in the KEK machine bodes well for upcoming data-taking.

The colliding beam energies are asymmetric so the $\Upsilon(4S)$ is boosted along the beam direction. This results in the daughter B mesons also being boosted, with $\beta\gamma \approx 0.4$, separating the two B meson decay vertices in the detector. The boost introduces some asymmetry in the design of the experiment. A cross-section of the

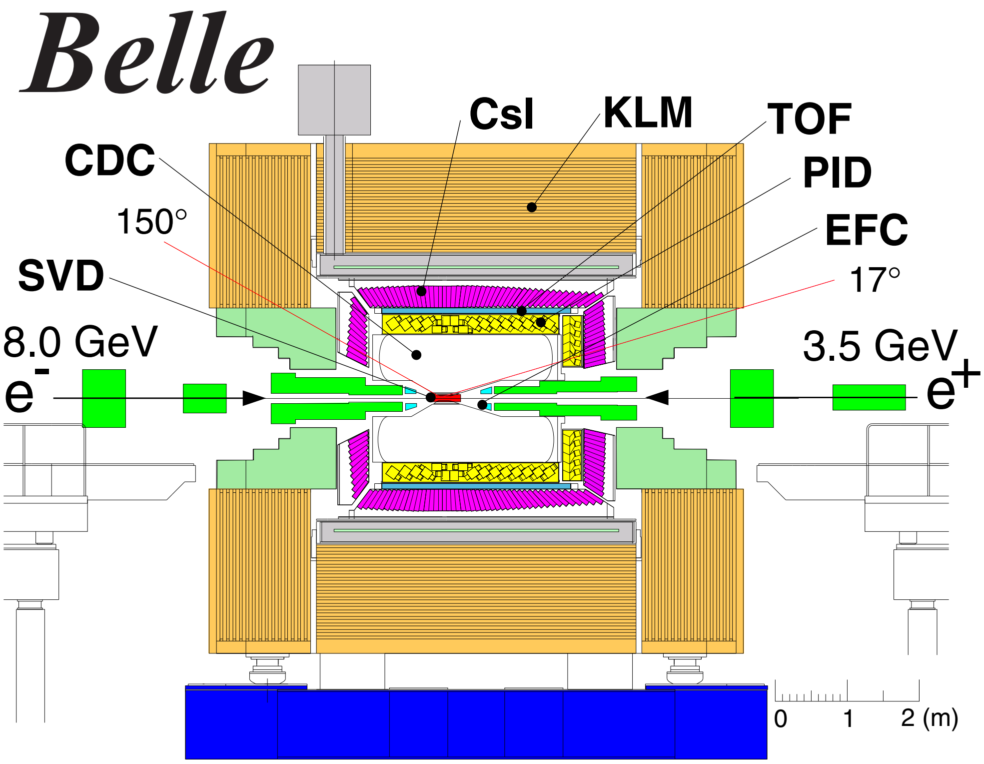

Figure 3: An elevation view of the Belle experiment.

cylindrical Belle detector is shown in fig. 3. The detector elements are arranged asymmetrically around the interaction point to improve the acceptance for B meson decay products.

Working outwards from the collision point B meson decay products encounter a three layer silicon vertex tracker that measures charged particle trajectories with 55 μm precision (at 1 GeV/c) and produces about 100 μm precision in z on the B decay vertices. They next pass through a Helium filled drift chamber that measures track momenta with a precision of $\sigma_p/p = (0.2p \oplus 0.3)\%$ providing excellent mass resolution for decays into charged tracks. This is followed by an Cesium-Iodide crystal calorimeter that has better than 2% energy resolution for 1 GeV photons. Belle includes a particle ID system that includes an aero-gel Cerenkov counter and a time of flight system that can distinguish kaons from pions up to 3.5 GeV/c with 90% efficiency and fake rates of less than 5%. This is followed by the solenoid coil and then a K_L^0 and muon detection system that identifies muons with less than 2% fake rate above 1 GeV/c. As a hadron absorber it also detects K_L^0 showers with an angular resolution of a few degrees.

The Belle detector has operated reliably over the first two years of KEK-B

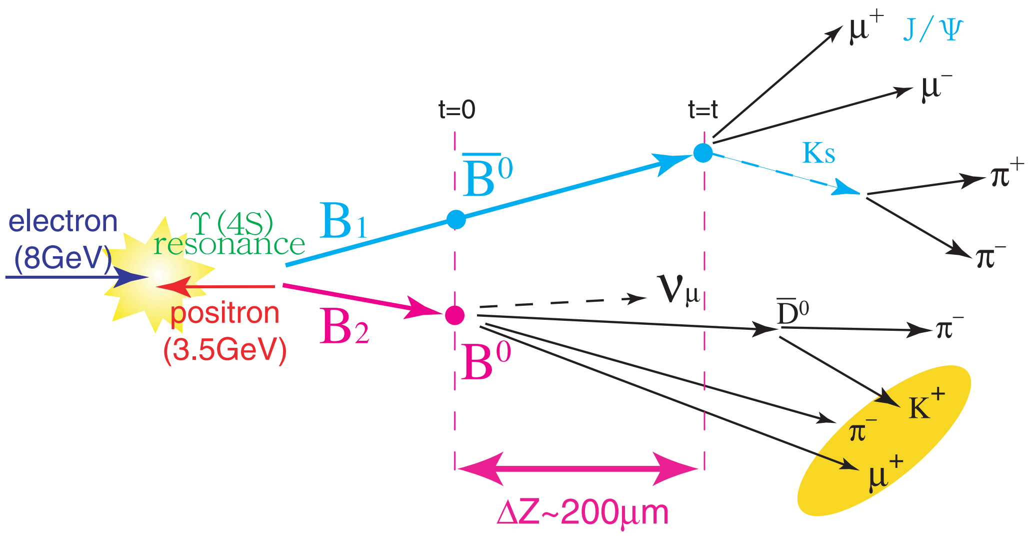

Figure 4: A schematic view the ingredients necessary to observe CP violation in B meson decay at an asymmetric e^+e^- collider.

operation, accumulating almost 78 fb^{-1} at the $\Upsilon(4S)$ resonance corresponding to over 84 million $B\bar{B}$ pairs that can be used for the study of CP violation in B decay. More details can be found in reference[3]

3 The Measurement of $\sin 2\phi_1$

There are three main ingredients that go into the measurement of a CP violating phase – for example $\sin 2\phi_1$ in $J/\psi K^0_S$ decay – at Belle. These are illustrated in fig. 4. First one must identify the decay vertices of the two B mesons. Second, since the final state we are studying is a CP eigenstate, we must tag the flavour of the other B meson as it decays. Since the $\Upsilon(4S)$ decay products evolve in a coherent $J = 1$ state, the decay of one of the B mesons into a B^0 (in the example shown in fig. 4) projects the other B meson into the $\bar{B}^0$ state. Finally, one must identify a sample of candidates which are CP eigenstate – $J/\psi K^0_S$ in this case. I will briefly describe each of these aspects of the measurement in the following sections.

3.1 B Meson Decay Vertexing

Identifying and separating the two B decay vertices on an event-by-event basis in Belle is a subtle process. Despite the boost from the asymmetric beam energies

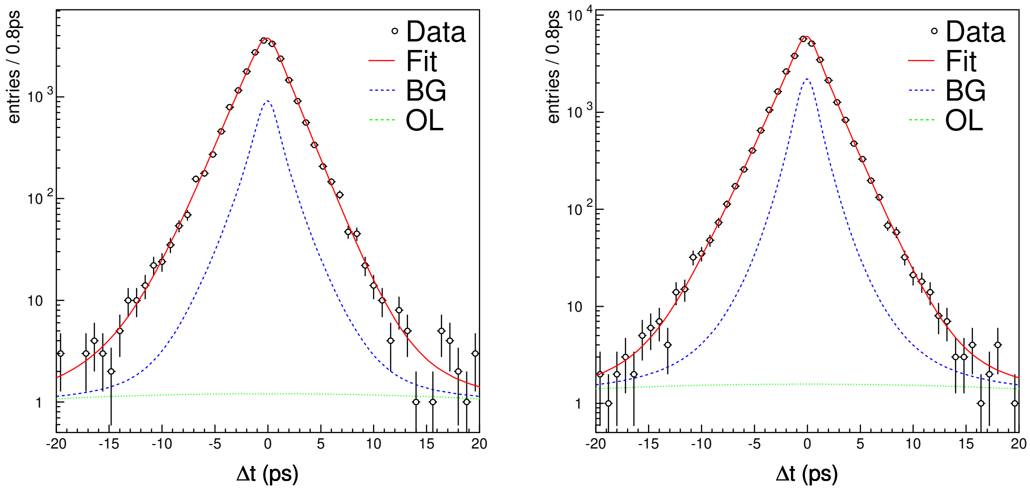

Figure 5: Left: The distribution of decay time differences between B^0 and $\bar{B}^0$ mesons measured by the Belle experiment. The open circles are the data, the solid line is the result of a maximum likelihood fit that includes a component proportional to the lifetime, and two components (dashed and dotted) that parametrise the detector resolution. Right: The distribution of decay time differences between B^+ and B^- mesons.

the B mesons only travel a few hundred microns ($\gamma c\tau \approx 250\mu$m) before they decay. The silicon vertex detector in Belle is measures the decay vertices with a precision of about 100 μm. A $J/\psi K_S^0$ decay vertex is typically determined with a precision of 75 μm, slightly better than the flavour tag B decay (at 140 μm) because there are generally more reconstructed tracks attached to the former vertex.

The precision of Belle's vertexing is demonstrated by our B lifetime measurement (shown in fig. 5) where one sees a clear difference between our detector resolution (dashed line) and the longer lived B meson decays (solid line through the data points). These fits allow us to make precise measurements of the charged and neutral B meson lifetimes and giving the ratio: $\tau_+/\tau_0 = 1.09 \pm 0.03$.[4] The detector resolution is understood beyond 10 B lifetimes and over 3 orders of magnitude in B decay rate. This is one of the crucial ingredients in being able to measure CP violation

3.2 Flavour Tagging in B^0 Meson Decay

A second key ingredient is being able to tag the flavour of the B meson opposite the CP eigenstate in the $B\bar{B}$ decay. We do this without fully reconstructing the

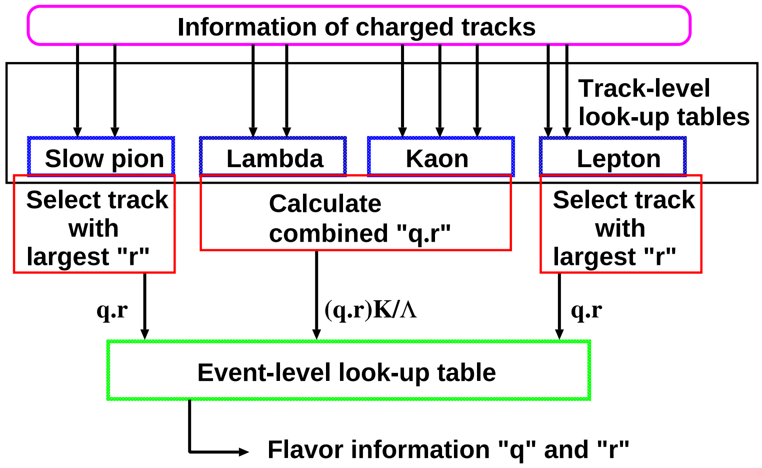

Figure 6: A schematic view of the Belle B^0 flavour tagging algorithm. Events are classified according to according to characteristics of the event: charged leptons, kaons, lambdas and slow pions. This information is sifted through a set of look-up tables (based on MC simulation) to identify and quantify the most reliable flavour tagging information in each event. The result of this procedure is the assignment of a "charge", q, and the reliability of this assignment, r.

opposite B – which would result in a significant loss in efficiency. Instead we look for characteristics of the other B decay that tag its flavour. For example, high momentum leptons are indicative of a direct semi-leptonic B decay, in which case the charge of the lepton is a direct indication of the flavour of B. Lower momentum leptons arise from a cascade semi-leptonic decay where the B meson first decayed to a charm meson and the latter decayed semi-leptonically. This results in the opposite correlation between the lepton charge and B meson flavour. Such information is combined in a set of look-up tables shown in fig. 6 that classify potential flavour information according to the sign of the b quark charge, q, and the reliability of the tagging information, r.

While the look-up table information – q, r and their correlations when more than one piece of tagging information is available in a single event – is extracted from a Monte Carlo simulation, the tagging algorithm is calibrated on a data control sample. Using a sample of $B \to D^* l\nu$ decays – where one knows the flavour of the B meson in each case, from the charge of the lepton in the final state – we measure the B mixing parameter from the time-dependence of the observed decays. We use our flavour tagging algorithm, described above, to classify them into

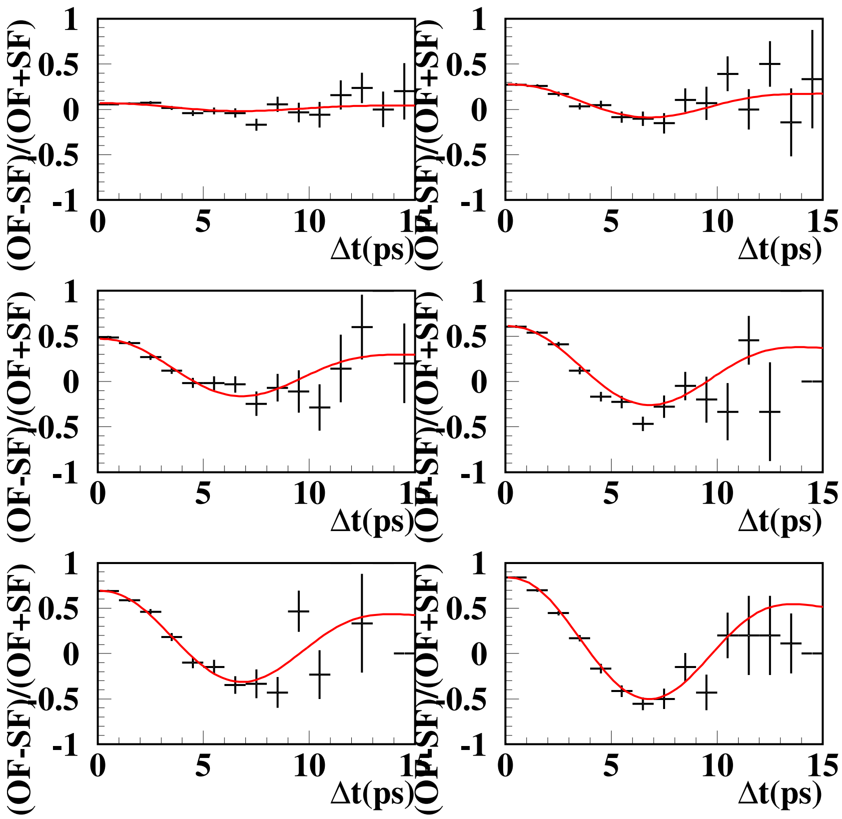

Figure 7: B mixing measurements in self-tagged $B^0 \to D^{*+} l^- \nu$ samples. This sample calibrates our tagging efficiency. The amplitude of the mixing observed depends on the reliability of the tag, which increases from top-left to bottom-right in this series of plots.

six different ranges of r, shown in fig. 7. One sees that the observed amplitude of the mixing oscillation is much less in the sample that is tagged with low reliability (top left) while the amplitude of the oscillation (at $\Delta t = 0$) almost reaches 1 for those events that our algorithm tags with the highest reliability (bottom right).

Figure 8 shows the correct tag probability from the six plots in fig. 7 versus the average r for each sample. The correct tag probability, $1 - 2w_r$, is extracted from w_r – the probability that a tag gives the wrong charge sign. In cases were w_r approaches 0.5 (a 50-50 guess at the charge of the b quark involved) the probability of tagging the B meson decay goes to 0. Conversely, when w_r goes to 0, one approaches a 100% correct tag probability. Figure 8 shows a strong correlation between our tagger's reliability, r and the correct tag probability as measured in

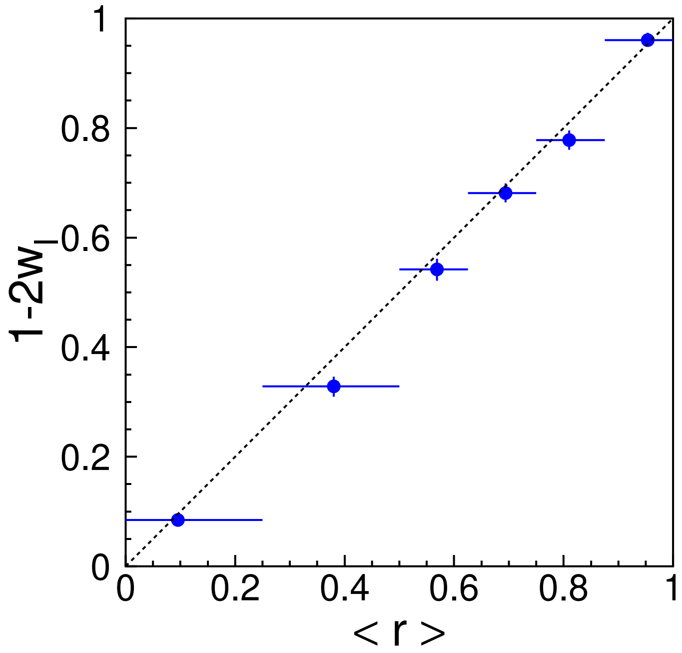

Figure 8: The correct tag probability $(1-2w_l)$ versus tag reliability, r. The wrong-tag fraction (w_l) is measured from the observed mixing in self-tagged B^0 samples (see fig. 7). The measured tagging probabilities $(1-2w_l)$ are used to weight the flavour determination in fits to CP eigenstates.

our control sample. We use these measured tag probabilities to weight our CP eigenstate decays when extracting their decay asymmetry.

With this algorithm we extract some tagging information from 99.5% of all B decay candidates. While some of the events have tags with low reliability, we measure an overall tagging efficiency of $28.8 \pm 0.6\%$, corresponding to almost 1/3 of our B sample being perfectly tagged. This represents an improvement from an effective tagging efficiency of $27.7 \pm 1.2\%$ in previous measurements[3] arising from improvements to our low-momentum track reconstruction efficiency and an improved silicon alignment – allowing us to associate more tracks with the tagging B decay vertex.

3.3 CP Eigenstate Event Samples

From a sample of 78 fb^{-1} of data taken at the $\Upsilon(4S)$ resonance between summer 2000 and summer 2002 Belle has a sample of almost 3000 $c\bar{c}K$ decay candidates. These are summarised in table 1 where one sees that about 1/3 of the candidates

Mode	CP (ξ_K)	Candidates	Purity (%)
$J/\psi K^0_S(\pi^+\pi^-)$	-1	1116	98
$J/\psi K^0_S(\pi^0\pi^0)$	-1	162	82
$\psi(2S)K^0_S$	-1	172	93
$\chi_{c1}K^0_S$	-1	67	96
$\eta_c K^0_S$	-1	122	68
$J/\psi K^{*0}(K^0_S\pi^0)$	1 (81%)	89	92
$J/\psi K^0_L$	1	1230	63
Total		2958	

Table 1: Summary of the CP candidates used to measure $\sin 2\phi_1$.

come from $J/\psi K^0_S$ decays where the K^0_S is reconstructed in a $\pi^+\pi^-$ final state. This golden mode also has the highest purity. There are a number of other modes that contribute to the measurement of $\sin 2\phi_1$ with other $c\bar{c}$ resonances and other K^0_S final states. Finally, a little over 1/3 of our sample is in the form of $J/\psi K^0_L$ decays that have the opposite CP eigenvalue. This sample provides an important cross-check of our results – helping to demonstrate the absence of a systematic offset in our measurement. Figure 9 shows the mass distribution for our candidates with K^0_S candidates in the final state.

While our K^0_L detector does not measure the energy of the hadronic shower of a neutral Kaon decay with high precision it measures the direction of such a shower with an accuracy of a few degrees. Having fully reconstructed a J/ψ meson one can hypothesize that a $B^0 \to J/\psi K^0_L$ decay has occurred and infer the magnitude of the K^0_L momentum, having measured on the K^0_L direction, by constraining the two body system (J/ψ, K^0_L) to the B^0 mass. Imposing this constraint reduces the number of handles one has to reject background but still provides one degree of freedom – chosen to be the momentum of the hypothetical B^0 candidate in $\Upsilon(4S)$ centre of momentum (shown in fig. 10). Successfully reconstructed $J/\psi K^0_L$ candidates peak near $p_B^{\rm cms} \approx 0.3$ GeV/c, while backgrounds generate a flatter distribution in $p_B^{\rm cms}$. From the distribution in fig. 10 we extract 1330 candidate events and estimate their purity to be 63%. Since many of the backgrounds under the $J/\psi K^0_L$ peak result from other B meson decays care must be taken when

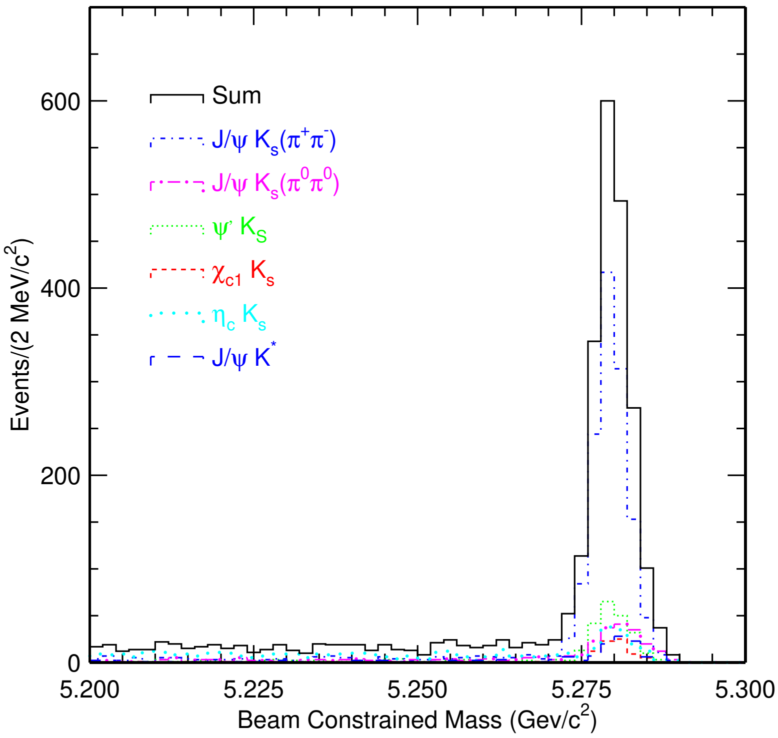

Figure 9: The beam constrained mass for the various different $\bar{c}cK^0_S$ final states used to measure indirect CP violation in B^0 decay at Belle. The largest sample comes from the $J/\psi K^0_S(\pi^+\pi^-)$ decays (dot-dashed line). The other modes combine to make up about 35% of our sample.

extracting a CP asymmetry from this sample to account for the CP asymmetry of the background. Our ability to do this is reflected a systematic uncertainty on our measurement.

3.4 Results

We perform a maximum likelihood fit to all our $c\bar{c}K$ candidates to extract their time dependent asymmetry (cf. equation 1). This fit includes the flavour tagging probability, uncertainties on the measured separation between the two B meson decays (converted to Δt using the B meson boost) as well as the purity of the signal for each type of decay – $J/\psi K^0_S(\pi^+\pi^-)$ candidates receive the highest weight because they tend to be cleaner (see table 1).

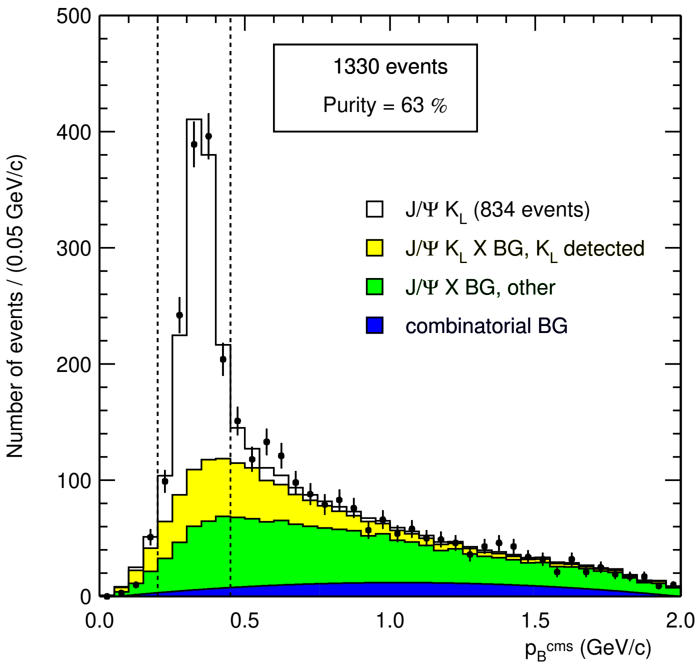

Figure 10: The centre of mass momentum distribution for Belle's $J/\psi K_L^0$ candidates used to measure indirect CP violation in B^0 decay at Belle. The signal forms a peak at $p_B^{\rm cms} = 0.33$ GeV/c, while backgrounds – where one or more final state particles have not be properly included in the B^0 candidate reconstruction, have their momentum smeared out to larger momenta.

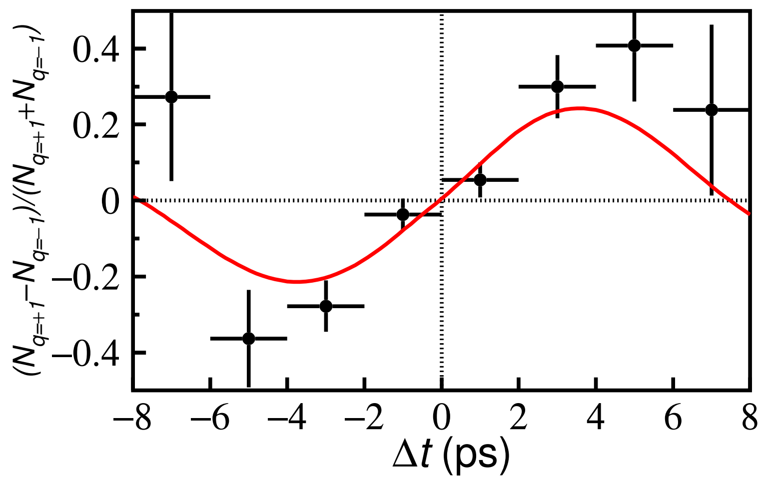

Figure 11: The time dependent asymmetry between B^0 and $\bar{B}^0$ decays to $\bar{c}cK_S^0$ final states ($\xi_{\rm CP} = -1$). The amplitude of this oscillation, extracted from an event-by-event maximum likelihood fit gives $\sin 2\phi_1 = 0.716 \pm 0.083$.

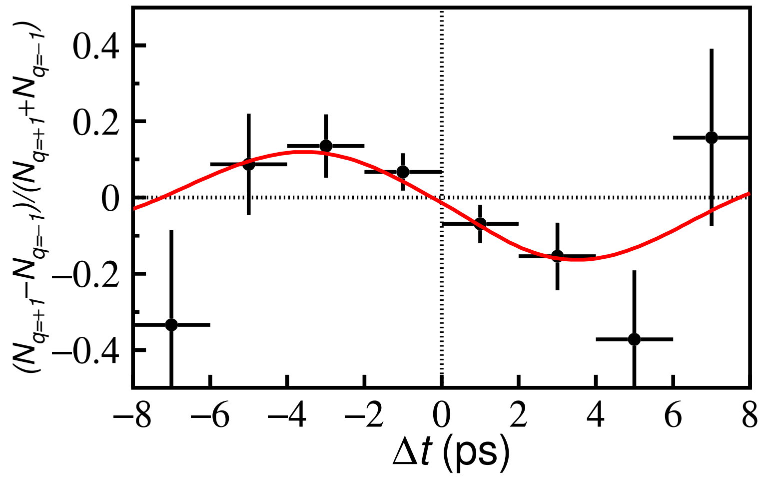

Figure 12: The time dependent asymmetry between B^0 and $\bar{B}^0$ decays to $J/\psi K_L^0$ final states ($\xi_{\rm CP} = 1$). The amplitude of this oscillation, extracted from an event-by-event maximum likelihood fit gives $\sin 2\phi_1 = 0.781 \pm 0.167$.

We first perform this fit separately for candidates with $CP = -1$ (the bulk of our data) and $CP = +1$ (our $J/\psi K_L^0$ sample), shown in figs. 11 and 12, respectively. We find the magnitude of the fit asymmetries are equal, but they have opposite sign – as expected. The fit results are reported in table 3. We then combine all candidates into a single fit (see fig. 13) – inverting the sign of Δt for the $CP = +1$ candidates – and obtain:

$$\sin 2\phi_1 = 0.719 \pm 0.074$$

The systematic uncertainties involved in this measurement are listed in table 2. The largest of these uncertainties are derived from measurements with our control data samples – for example the flavour tagging discussed in section 3.2 – and thus can be expected to be reduced as more data becomes available. More details on this measurement can be found in reference.[5] The overall systematic uncertainty is small compared to the statistical precision which bodes well for future measurements.

3.5 Cross-checks of $\sin 2\phi_1$

We perform a number of cross-checks on non-CP eigenstate samples, all of which exhibit null asymmetries with statistical precisions ranging from 0.02 to 0.09. We do not include these as systematic uncertainties but they provide additional confidence in our main result. We have also sub-divided our data into different

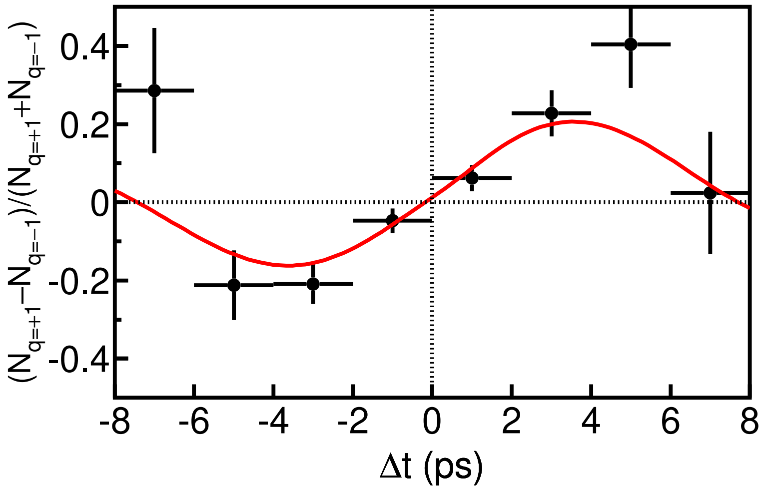

Figure 13: The combined time dependent asymmetry between B^0 and $\bar{B}^0$ decays to $\bar{c}cK^0$ final states (flipping the sign of the candidates with $\xi_{\rm CP} = 1$). An event-by-event maximum likelihood fit gives $\sin 2\phi_1 = 0.719 \pm 0.074$.

sub-samples to see whether there is any evidence for systematic variations in our result. Finding none (see table 3) gives us further confidence in our main result. We do not ascribe additional systematic uncertainty for these variations as they are all consistent with our quoted result within the expected statistical variation from the smaller sub-samples involved in the cross-checks.

4 CP Asymmetries in $B^0 \to \pi^+\pi^-$ Decay

Having observed indirect CP violation in $B \to J/\psi K$ decays it is natural to study other CP eigenstates. The decay $B^0 \to \pi^+\pi^-$ is interesting because there are at least two important amplitudes that interfere in the direct decay. These amplitudes are show diagrammatically in fig. 14. With more than one amplitude in the direct decay path one can have a $\cos \Delta m \Delta t$ dependence in the CP asymmetry. This dependence comes from the interference of the two direct decay amplitudes and can appear in addition to the $\sin \Delta m \Delta t$ time-dependence from the interference with the mixing amplitude:

$$\begin{aligned} A_{CP}(\Delta t) &= \frac{\frac{dN}{dt}(\bar{B}^0 \to F_{\rm CP}) - \frac{dN}{dt}(B^0 \to F_{\rm CP})}{\frac{dN}{dt}(\bar{B}^0 \to F_{\rm CP}) + \frac{dN}{dt}(B^0 \to F_{\rm CP})} \\ &= S_F \sin\ \Delta m \Delta t + A_F \cos\ \Delta m \Delta t \qquad [2] \end{aligned}$$

The measurement of the $B^0 \to K^+\pi^-$ branching fraction – three times larger than the $B^0 \to \pi^+\pi^-$ branching fraction – is strong evidence that the penguin

Uncertainty Source	Value
Vertexing Reconstruction	0.022
Flavour Tagging	0.015
Vertex Resolution	0.014
Fit parametrisation	0.011
$J/\psi K_L^0$ Background	0.010
Δm_d, τ_B	≤ 0.010
Total	0.035

Table 2: Systematic uncertainties on the measurement of $\sin 2\phi_1$.

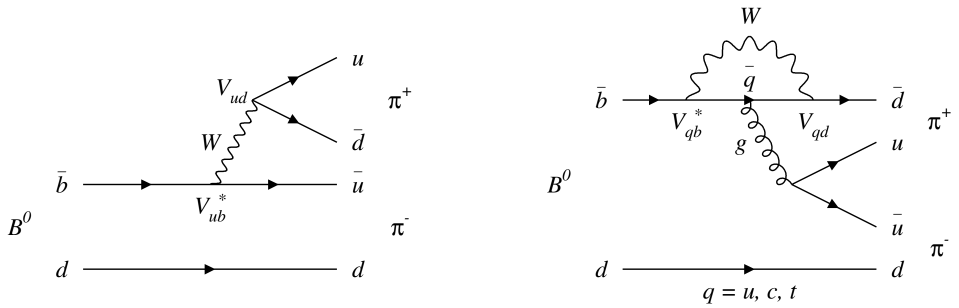

Figure 14: Two tree level diagrams for $B^0 \to \pi^+\pi^-$ decays. Given that there are two paths to the same CP eigenstate, their interference can produce direct CP violation in this mode.

amplitude (right diagram in fig. 14) is not small. In $B \to \pi\pi$ decay the V_{CKM} elements involved relate this this asymmetry to the angle ϕ_2. However the penguin diagram can introduce a non-CKM phase thus:

$$S_F \approx \sin(2\phi_2 + \theta)$$

where θ can come from the gluon in the penguin process. While waiting for measurements of the various $B \to \pi\pi$ branching fractions (see reference[6]) with sufficient precision to be able to measure θ, it is still interesting to measure the $\pi^+\pi^-$ asymmetry and perhaps get some hint of the size of the combination $2\phi_2+\theta$.[7]

Subsample (stat error only)	
$J/\psi K^0_S(\pi^+\pi^-)$	0.73 ± 0.10
$(c\bar{c})K^0_S$ (except $J/\psi K^0_S(\pi^+\pi^-)$)	0.67 ± 0.17
$J/\psi K^0_L$	0.78 ± 0.17
$f_{tag} = B^0$	0.65 ± 0.12
$f_{tag} = \bar{B}^0$	0.77 ± 0.09
$r \leq 0.5$	1.26 ± 0.36
$0.5 \leq r \leq 0.75$	0.62 ± 0.15
$0.75 \leq r$	0.72 ± 0.09
All	0.72 ± 0.07

Table 3: Cross-checks of $\sin 2\phi_1$ from fits to subsets of the data.

4.1 $B^0 \to \pi^+\pi^-$ Candidate Selection

The candidates and result presented here is from 43 fb^{-1} of data collected by the Belle experiment. Further details can be found in reference.[8] While the B vertexing and flavour tagging described in sections 3.2 and 3.1 can be used in a measurement of the $\pi^+\pi^-$ asymmetry, the candidate selection here is more challenging. The branching fractions for $B \to h^+h^-$ are an order of magnitude smaller than for the $J/\psi K$ final states – on the order of 10^{-5}. Furthermore the $B \to \pi^+\pi^-$ decays have only two, relatively high momentum, tracks in the final state – making these candidates look more like the $e^+e^- \to q\bar{q}$ continuum background. Belle uses a set of event-shape moments (Fox-Wolfram moments) and the reconstructed B^0 candidate direction to suppress continuum background. Figure 15 shows the distribution of R, our continuum suppression variable for $B\bar{B}$ data (open circles) and off-resonance data (closed circles). By requiring $R > 0.8$ we reduce the continuum background by an order of magnitude while retaining two third of our B candidates.

Since these events are fully reconstructed we are able to measure both the beam-constrained mass, m_{bc}, and the difference between the reconstructed energy of the B candidate and the beam energy. Figure 16 shows the distributions of both of these variables for our $B \to h^+h^-$ sample. Comparing the $\mathrm{m_{bc}}$ distribution

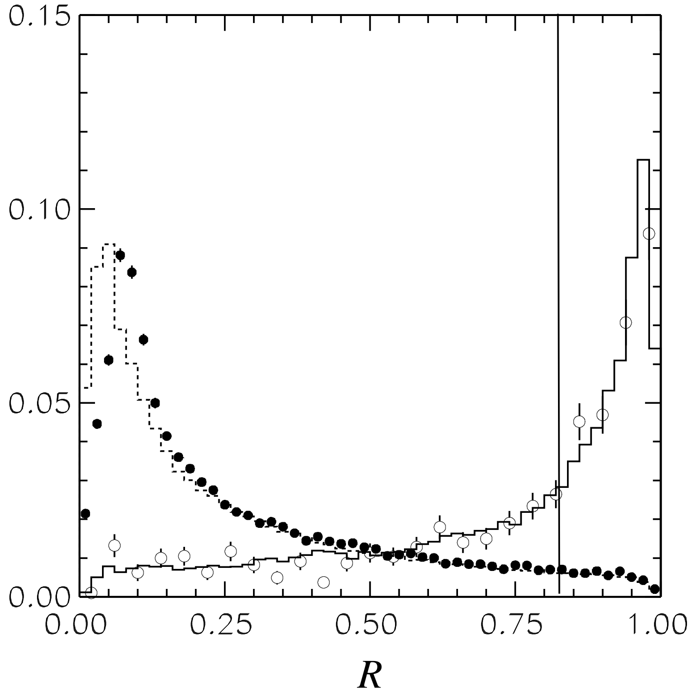

Figure 15: Low multiplicity final states are subject to higher background from events produced from the e^+e^- continuum. To suppress these Belle combines event shape variables to get an overall likelihood, R. The solid points are continuum data, while the open points are a control sample of fully reconstructed, low-multiplicity B candidates. $B^0 \to \pi^+\pi^-$ candidates are required to $R > 0.8$.

for these candidates to that of the $J/\psi K$ candidates in fig. 9 one sees that the background is much more prominent. In the ΔE distribution (on the right in fig. 16) one can see the source of these backgrounds. The remaining continuum background populates ΔE almost uniformly – falling somewhat at higher ΔE due to phase space – and is represented by the dotted line. B decays to three or more particles, where we have missed one in our reconstruction populate the low ΔE region (grey line) at a much lower rate than the continuum. Finally, $B \to K^+\pi^-$ candidates that have not been rejected by our particle identification produce a small peak at $\Delta E \approx -0.045$ GeV. This peak is shifted because these candidates have been reconstructed assuming that both B decay daughter tracks are pions (with a mass of 140 MeV/c^2), if one of them is really a kaon (with a mass of 500 MeV/c^2) then the reconstructed energy shifts down by 45 MeV. These background events are represented in our fit by the dot-dashed line.

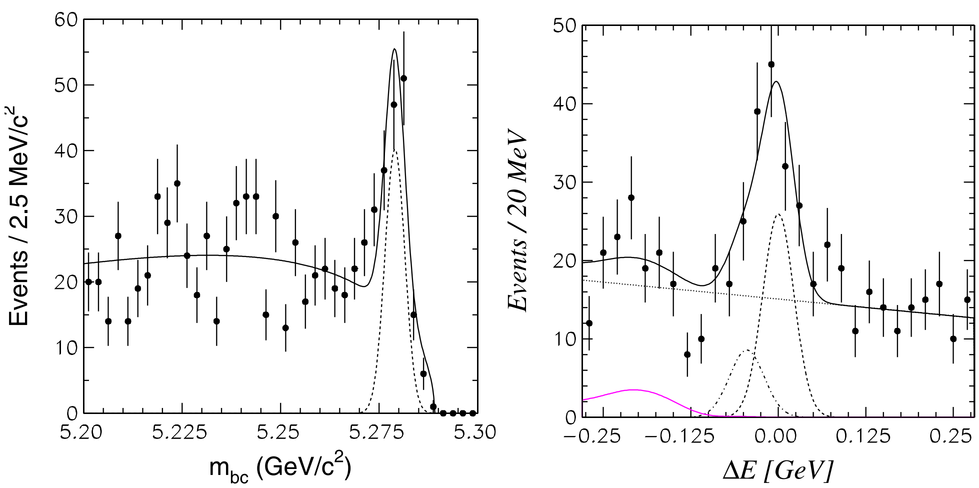

Figure 16: Left: The beam constrained mass, $\mathrm{m_{bc}}$, for the $B^0 \to \pi^+\pi^-$ candidates used to extract the CP asymmetry. Right: The energy difference distribution, ΔE, for the same candidates. In Δe the $\pi^+\pi^-$ signal peaks at 0 (dashed Gaussian), the $K^+\pi^-$ background peaks at -0.045 GeV (dot-dashed Gaussian). The continuum is parametrised as a falling linear background (dotted line) while B^0 decays with more that two particles in the final state appear at low ΔE.

We restrict our CP fit to candidates that have $|\Delta E| < 0.067$ GeV, eliminating the mis-reconstructed B background entirely and leaving us with 74 $\pi^+\pi^-$ candidates, 28 $K^+\pi^-$ candidates and about 100 candidates that come from the e^+e^- continuum.

4.2 The CP Fit

We perform an event-by-event likelihood fit to the time dependent asymmetry for the $B \to \pi^+\pi^-$ candidates. In order to maximise our sensitivity to the $\pi^+\pi^-$ asymmetry this fit weights the events according to their continuum likelihood (events near $R = 1$ are weighed more heavily) as well as their flavour tagging probability and vertex reconstruction quality – as was done for $\sin 2\phi_1$.

Figures 17 a) and b) show the Δt distributions for events tagged as coming from B^0 and $\bar{B}^0$ decays, respectively. The continuum and $K^+\pi^-$ backgrounds are represented by the dashed lines centered at $\Delta t = 0$ in each case. The hatched areas in each plot are what the fit ascribes to having come from $B \to \pi^+\pi^-$ candidates. The sum of these two distributions give the solid line which fits the data points. Figure 17 c) shows the Δt distribution for just the $B \to \pi^+\pi^-$ component of the fit. Here we see that our fit predicts that there are almost twice as many B^0

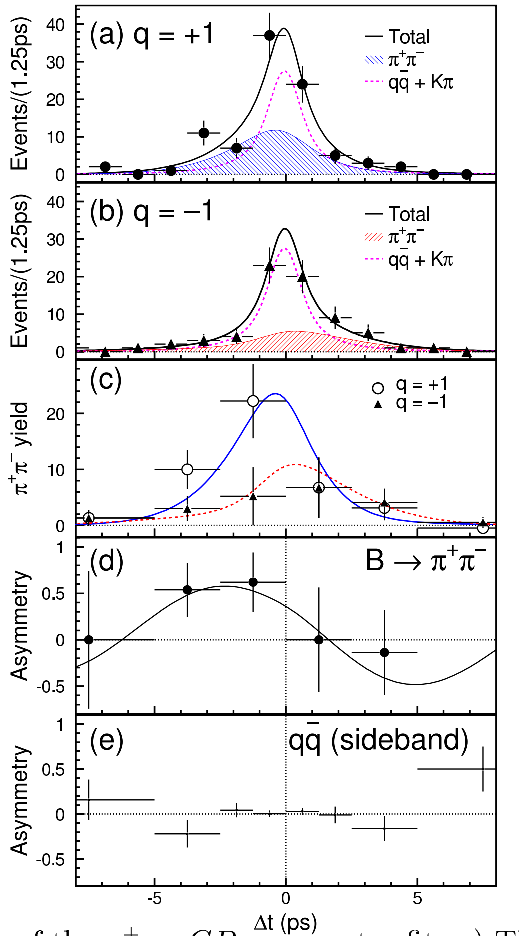

Figure 17: The results of the $\pi^+\pi^-$ CP asymmetry fit. a) The Δt distribution for candidates tagged with $q = 1$. The signal is shown as the hatched region, while the background (dominated by the continuum) is shown by the dashed line. The solid line is a projection of the overall fit and the solid points are the data. b) The Δt distribution for candidates with tagged $q = -1$. c) The circles (triangles) are the background subtracted data for $q = (-)1$ while the curves are fit projections for the two flavours. d) The difference between the two data-samples in c). e) The asymmetry observed in a continuum data sample.

candidates and $\bar{B}^0$ candidates in our sample – independent of Δt, an indication of direct CP violation. Finally, fig. 17 d) shows the asymmetry between the two distributions in fig. 17 c). Here one sees an asymmetry leading to our fit result:

$$\begin{aligned} S_{\pi\pi} &= -1.21^{+0.38}_{-0.27}(\text{stat})\,^{+0.16}_{-0.13}(\text{sys}) \\ A_{\pi\pi} &= 0.94^{+0.25}_{-0.31}(\text{stat})\pm 0.09(\text{sys}). \end{aligned}$$

This is three sigma evidence for both direct CP violation in the decay $B \to \pi^+\pi^-$ and indirect CP violation. More details can be found in reference.[8]

We have performed a large number of cross-checks on this fit, including fits to the $B^0 \to K^+\pi^-$ sample which should not have a CP violating asymmetry, fits to continuum side-bands (see fig. 17 e)) that are not expected to exhibit any asymmetry. None of these fits show significant asymmetries. We have simulated the size of our statistical uncertainties. We find that our statistical uncertainty on $S_{\pi\pi}$ is somewhat smaller than we might have expected for a sample this size. Still there is a 5% chance that we might have gotten a smaller uncertainty. While unlikely, this is not an unacceptable statistical fluctuation. Finally, we have performed a series of toy Monte Carlo simulations, each generated with $(S_{\pi\pi}, A_{\pi\pi}) = (0,0)$ and sample sizes (signal and background) that mimic those in our data. We find that 1.6% of these toy Monte Carlo samples return a fit value farther from $(S_{\pi\pi}, A_{\pi\pi}) = (0,0)$ than our data.

5 CP Asymmetries in Rarer B^0 Decay Modes

Having looked at two of the more plentiful B meson decays that are CP eigenstates, we have also looked at the next generation, of B decay modes where one might hope to extract CP phases. One such class of decays is shown in fig. 18. With no tree level contribution these decay processes might be expected to have branching fractions at least as small as those discussed above. In fact, the mode $B \to \eta' K_S^0$ has a branching ratio that is somewhat larger than the mode $B \to \pi^+\pi^-$ and clearly larger than the, as yet unseen, decay $B \to \eta K$. That the $\eta' K$ branching ratio is so large (about 5×10^{-5}) is not easy to understand theoretically – hinting that there may be more that just a charged W boson involved in the loop at the top of the diagram. If there were contributions from a charged Higgs to this amplitude, it would be likely to introduce an additional phase, interfering with those predicted by the CKM model. In the absence of such new phases this decay would provide another way – albeit a much lower statistics way – to measure $\sin 2\phi_1$. Thus a comparison of the CP asymmetry in $\eta' K_S^0$ decays with that seen in $J/\psi K_S^0$ decays could help unravel the mystery of the large branching of B mesons into this final state and may provide a glimpse of physics beyond the Standard Model.

5.1 CP Asymmetry in the Decay $B^0 \to \eta' K_S^0$

Figure 19 shows the mass distribution for 128 candidate $B^0 \to \eta' K_S^0$ decays from 78 fb^{-1} of Belle data. Here the η' candidates have been reconstructed in $\eta\pi^+\pi^-$

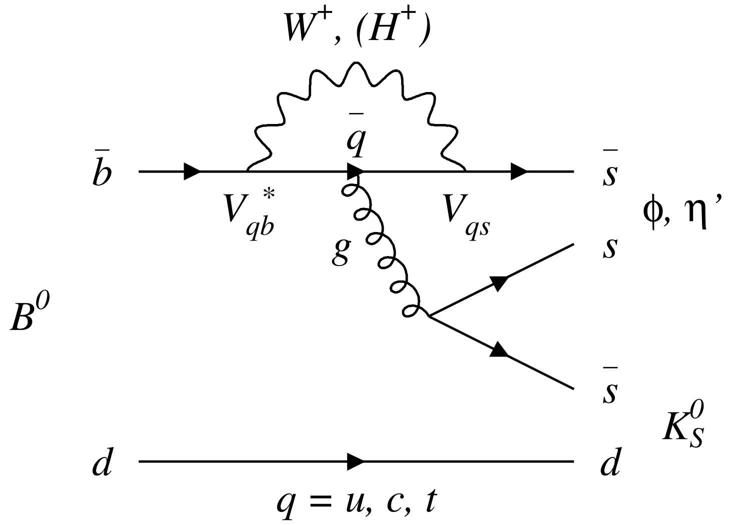

Figure 18: The Feynman-diagram for the decay $B^0 \to \eta' K^0_S$. The unexpectedly large branching fraction into this mode hints that there may be extra contributions to the amplitude – which could introduce additional CP violating phases.

and $\rho^0\gamma$ intermediate states and then combined with K^0_S candidates reconstructed from $\pi^+\pi^-$ combinations. The plot on the right of fig. 19 shows the $B^0\bar{B}^0$ asymmetry, as a function of Δt, where the candidates have been flavour tagged and vertexed in the same way as our $J/\psi K^0_S$ candidates described above. The coefficient of for the indirect CP violation derived from this fit (see eqtn. [2], with A constrained to 1) is listed in table 4. While the statistics are still poor, this is a demonstration that we can measure CP asymmetries in these very rare modes. More details on this analysis can be found in reference[9] that describes this measurement made on the first 42 fb^{-1} of data shown here.

We perform the same measurements on samples of $B^0 \to K^+K^-K^0_S$ decays. Though the number of candidates in this sample is even smaller we can begin to probe their CP asymmetry. We separate the K^+K^- candidates into two samples. When $m_{K^+K^-} \approx m_\phi$ we know this final state has $CP = -1$ providing a potentially clean determination of $\sin 2\phi_1$. Unfortunately the statistics are still very limited. The remaining sample is somewhat larger, providing a more inci-

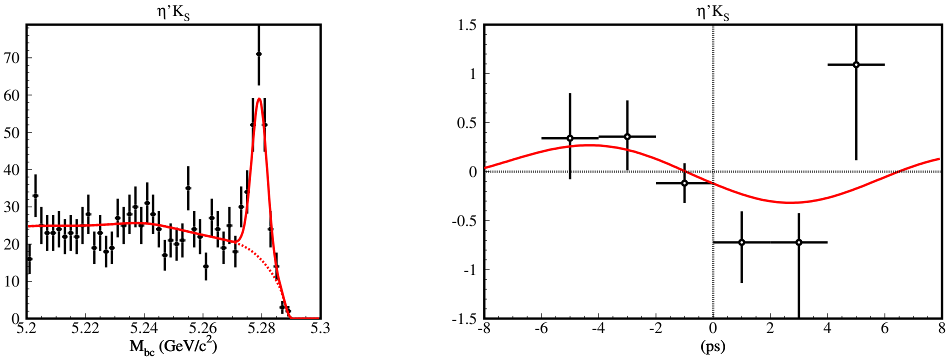

Figure 19: Left: The beam constrained mass distribution for $B^0 \to \eta' K_S^0$ candidates. Right: The CP asymmetry as a function of Δt for these candidates.

Mode	$(\sin 2\phi_1)_{\mathrm{eff}}$	Candidates
$\eta' K_S^0$	$0.76 \pm 0.36(\mathrm{stat}) \pm 0.06(\mathrm{sys})$	128
ϕK_S^0	$-0.73 \pm 0.64(\mathrm{stat}) \pm 0.18(\mathrm{sys})$	35
$(K^+K^-)_{\mathrm{non-res}} K_S^0$	$0.52 \pm 0.46(\mathrm{stat}) \pm 0.11(\mathrm{sys})^{+0.27}_{-0.03}(\mathrm{CP})$	95

Table 4: CP fit parameters for rare decay modes.

sive measurement of the CP asymmetry. Studies of decays related to this one by isospin ($B^+ \to K^+ K^0 \bar{K}^0$) have shown that this non-resonant sample is $97^{+3}_{-16}\%$ $CP = +1$. This bound on the CP symmetry of the K^+K^- non-resonant final state translates into the systematic on the effective $\sin 2\phi$ listed in table 4. Fortunately the measurement of the CP symmetry in these decays will improve with additional statistics so the non-resonant mode might eventually provide a clean measurement of $\sin 2\phi_1$ in this rare decay.

6 Summary and Future Prospects

Belle has studied the decay of B^0 mesons into a number of CP eigenstates. The most precise measurement of $\sin 2\phi_1$ to date is in the mode: $B^0 \to J/\psi K_S^0$. Most of the systematic uncertainties involved in that measurement come from calibrations of our flavour tagging and decay vertexing procedure on data control samples. Thus it is reasonable to expect that the precision on $\sin 2\phi_1$ – both statistical and systematic – will improve as more data becomes available. Figure 20 shows a prediction of how the precision on $\sin 2\phi_1$ will scale as Belle's integrated luminosity increases. The lowest curve shows the evolution of the systematic uncertainty on

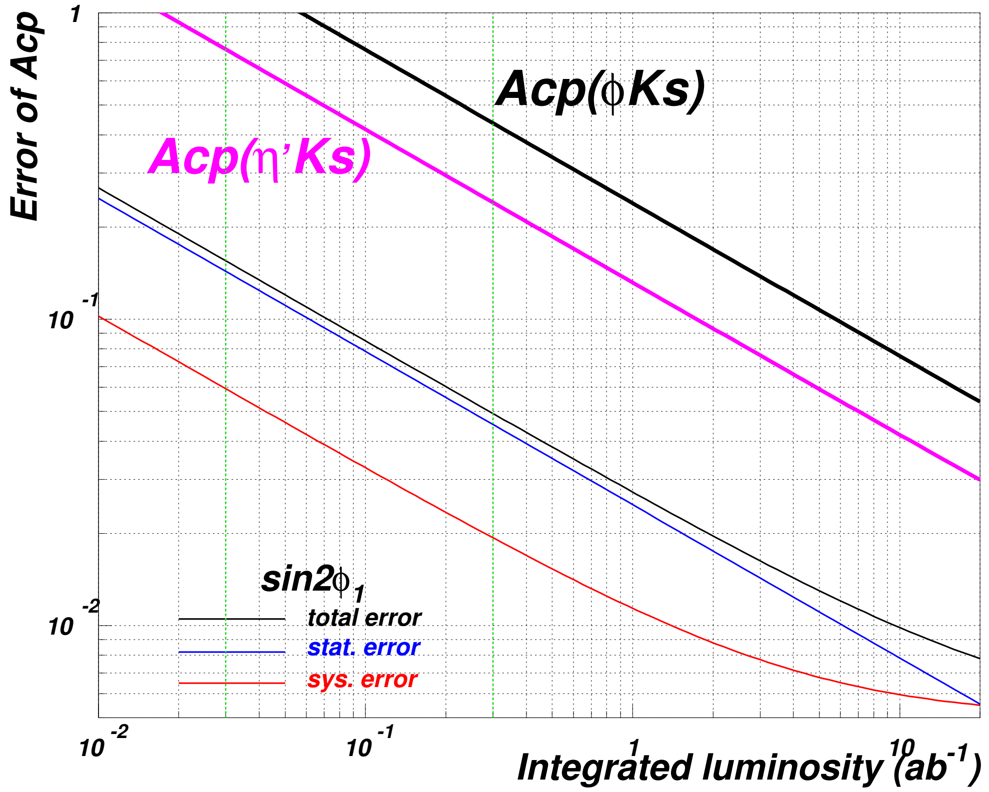

Figure 20: Prospects for improving the precision on $\sin 2\phi_1$ from the decay $J/\psi K_S^0$ (lower set of thin curves) with additional statistics. For comparison the precision expected on rarer modes ($\eta' K_S^0$ thick grey curve and ϕK_S^0 thick black curve) are also shown.

$\sin 2\phi_1$, in the $J/\psi K_S^0$ measurement. It should improve until as least 1000 fb^{-1} of data has been collected. At that point we expect an overall precision (uppermost thin line in fig. 20) of $\delta \sin 2\phi_1 \approx 0.025$.

The rarer modes will also benefit from the increase in statistics. Belle expects to be able to accumulate 1 ab^{-1} of data in the next 3 or 4 years. At that point the precision on the $\eta' K_S^0$ asymmetry should approach the precision that we currently have on the $J/\psi K$ asymmetry. If there are other modes contributing to the phase in $\eta' K_S^0$ decays nature would have been required to perform some un-natural fine-tuning for our precision not to show some discrepancy between what would otherwise be two measurements of the same quantity.

The B factories were built to confirm the CP violation predicted by the CKM model in B^0 meson decay – they have now achieved that milestone. Having made a 10% measurement of $\sin 2\phi_1$ in the golden mode: $J/\psi K_S^0$, they are now pushing to improve the precision to a few percent. At the same time they are expanding their scope to study other decay processes, and in doing so measure other angles (and sides) of the unitarity triangle. This will begin to over-constrain the CKM model and test whether there is physics beyond the three known families of quarks and their Standard Model electroweak decays. In the coming years the flavour sector will become ever more constrained reducing the room for speculation about the physics that explains why we have three families of quarks.

References

[1] M. Kobyashi and T. Maskawa, Prog. Theor. Phys. **49**, 652 (1973).

[2] A.B. Carter and A.I. Sanda, Phys. Rev. Lett. **45**, 952, (1980).

[3] K. Abe *et al.* (The Belle Collaboration), *Observation of Mixing-induced CP Violation in the Neutral B Meson System* , Phys. Rev. **D 66**, 032007 (2002).

[4] K. Abe *et al.* (The Belle Collaboration), *Precise Measurement of B Meson Lifetimes with Hadronic Decay Final States* , Phys. Rev. Lett. **88**, 171801 (2002).

[5] K. Abe *et al.* (The Belle Collaboration), *Improved Measurement of Mixing-induced CP Violation in the Neutral B Meson System* , Phys. Rev. **D 66**, 071102(R), (2002).

[6] B. Casey, these proceedings.

[7] M. Gronau and J.L. Rosner, *Strong and Weak Phases from Time-Dependent Measurements of* $B \to \pi\pi$, Phys. Rev. **D 65**, 093012 (2002).

[8] K. Abe *et al.* (The Belle Collaboration), *Study of CP-Violating Asymmetries in* $B^0 \to \pi^+\pi^-$ *Decays* , Phys. Rev. Lett. **89**, 071801 (2002).

[9] K.F. Chen, K. Hara *et al.* (The Belle Collaboration), *Measurement of CP-Violating Parameters in* $B \to \eta' K$ *Decays* , Phys. Lett. **B 546**, 196 (2002).